HYDROLOGICAL PROCESSES
Hydrol. Process. **30**, 2138–2152 (2016)
Published online 12 February 2016 in Wiley Online Library
(wileyonlinelibrary.com) DOI: 10.1002/hyp.10783

Field study on drainage densities and rescaled width functions in a high-altitude alpine catchment

Raphaël Mutzner,[1]* Paolo Tarolli,[2] Giulia Sofia,[2] Marc B. Parlange[3] and Andrea Rinaldo[1,4]

[1] *School of Architecture, Civil and Environmental Engineering, École Polytechnique Fédérale de Lausanne, Lausanne, Switzerland*
[2] *Department of Land, Environment, Agriculture and Forestry, University of Padua, Agripolis, viale dell'Università 16, 35020 Legnaro (PD), Italy*
[3] *Department of Civil Engineering, University of British Columbia, Vancouver, BC, Canada*
[4] *Dipartimento ICEA, University of Padua, via Loredan 20, I-35131 Padova, Italy*

Abstract:

This paper addresses the effect of accurately mapping spatially heterogeneous drainage densities in high-altitude alpine basins on Rescaled Width Functions (RWFs), used in some applications as a minimalist model of the hydrologic response. The channel network and 373 of its channel heads were mapped in the field in a high mountain catchment in the Swiss Alps. The mapped channel network is characterized by highly uneven drainage density, here described by the distribution of the length to the first channelized site computed along steepest descent from any unchannelled site. Various channel networks were extracted from a 1 m lidar-derived digital terrain model and compared with the field-mapped channel network using geomorphologic parameters, hillslope-to-channel distance and RWFs. Our results show that the channel network derived by statistical analysis of surface morphology is consistent with the field-mapped network. Larger discrepancies were observed when the channel network was obtained with classical threshold-based approaches relying on cumulative drainage area and local slope. The actual arrangement of the drainage densities has a significant impact on the RWFs. The discrepancy was largest between RWFs derived from classical extraction methods and RWFs derived with the field-mapped network, indicating an inappropriate extraction of the channelled portion of the high-altitude catchment that is a reflection of the variety of channel initiation processes. Our results suggest that spatial heterogeneity of the drainage density might play an important role in modelling streamflow generation.

KEY WORDS drainage density; DTM; rescaled width function; channel head; channel network

Received 15 October 2014; Accepted 23 December 2015

INTRODUCTION

The recent increased availability of remote-sensing techniques has led to new understanding of Earth surface processes. In particular, airborne and terrestrial LiDAR (Light Detection And Ranging) have been used to produce high resolution topographic maps, opening new opportunities for studying river and basin geomorphology (e.g. Jaboyedoff *et al*., 2012; Tarolli, 2014). LiDAR-derived Digital Terrain Models (DTMs) provide fine-scale knowledge of a watershed's geomorphology, which is crucial for environmental, agricultural and flood management applications. High-resolution DTMs also serve as a basis for modelling the hydrological response in poorly monitored basins (Beven, 2011) and are instrumental in describing shallow landsliding or debris flow (Simoni *et al*., 2008; Tarolli *et al*., 2012; Cavalli *et al*., 2013). In this context, spatially explicit hydrological models that describe the geomorphology accurately are often used to reproduce hydrographs (Szilágyi and Parlange, 1999; Schaefli *et al*., 2014; Singh *et al*., 2014; Comola *et al*., 2015). Among these is the Width Function Intantaneous Unit Hydrograph model, which is mainly based on the analysis of DTMs. In the Width Function Intantaneous Unit Hydrograph model, the width function, defined as the number of channelized pixels located at a distance from the outlet along the streams divided by the number of channelized pixels, is used as a probability density function of travel length (Kirkby, 1976; Troutman and Karlinger, 1985; Mesa and Mifflin, 1986; Gupta and Mesa, 1988). However, this approach does not take into account the hillslope travel length that might be valid only in large basins when the travel length in the basin is dominated by the channel network (D'Odorico and Rigon, 2003). Following the idea of Van der Tak and Bras (1990), Rinaldo *et al*. (1995) introduced the Rescaled Width Function (RWF), defined as the number of cells located at a distance L taken as the sum of flow path inside the river network L_c and the flow path across the hillslope L_h. In this approach, the hillslope flow path

*Correspondence to: Raphaël Mutzner, School of Architecture, Civil and Environmental Engineering, École Polytechnique Fédérale de Lausanne, Lausanne, Switzerland.
E-mail: raphael.mutzner@gmail.com

is amplified to account for smaller hillslope celerities compared with channel celerities.

The RWF formulation has been extensively used to analyse the contribution of hillslopes and channels to the hydrologic response (Botter and Rinaldo, 2003; D'Odorico and Rigon, 2003), for regionalization and scaling properties of storm hydrographs (Di Lazzaro, 2009; Di Lazzaro and Volpi, 2011) and to model the hydrological response during flood events (Giannoni *et al*., 2003; Borga *et al*., 2007; Zoccatelli *et al*., 2010). The RWF is also used to estimate a catchment's geomorphological instantaneous unit hydrograph by dividing the flow path inside the river network L_c and the flow path across the hillslope L_h by their respective celerities. Recent studies have proposed varying the hillslope celerity spatially, with local values depending on land use or topographic characteristics (Grimaldi *et al*., 2010; Grimaldi *et al*., 2012; Petroselli, 2012). However, the hillslope and channel celerities are usually assumed to be uniform within the catchment, and to be typically separated by an order of magnitude. They can be randomized and made nonstationary, yielding proper ensemble averages (Rinaldo *et al*., 1995).

The RWF relies on an accurate partitioning of the landscape into hillslope and channel network portions and is therefore eminently suited to studies that compare various distributions of the partitioning of the channel network derived from different extraction procedures. Surprisingly, few studies have addressed the impact of channel identification procedures on RWF. The simplest and most widely used method to automatically extract the channel network is to compute the contributing area of each cell of the DTM, i.e. computing the number of cells draining in each cell following the steepest path among the eight neighbouring cells. Then, a constant critical support area is chosen (e.g. O'Callaghan and Mark, 1984) as the criterion for channel initiation. Gandolfi and Bischetti (1997) analysed the effect of the area threshold on the geomorphologic instantaneous unit hydrograph, width function and geomorphological indices in two small alpine basins using DTMs with 10-m resolution. Their result showed that the choice of area threshold significantly impacts the hydrologic response modelling. Using the area threshold method, Nardi *et al*. (2008) assessed the impact of flow direction computation and flat area removal on the RWF and geomorphological parameters.

The second most widely used method to automatically extract the channel network is based on experimental data from Montgomery and Dietrich (1992). They proposed an empirical threshold for channel intiation depending on contributing area A and local slope S, in the form AS^k. Unlike the method based solely on contributing area thresholding, this method allows the drainage density to vary spatially; this is also its main advantage. Giannoni *et al*. (2005) proposed a procedure to objectively and automatically establish the AS^k threshold and studied the effect of the threshold on the hillslope path length frequency distribution and on the RWF.

The thresholds used for channel initiation are usually assumed to be constant on the catchment scale. However, several studies have shown that a unique threshold for channel head identification and channel network extraction might not exist at the catchment scale (Jaeger *et al*., 2007; Tarolli and Dalla Fontana, 2009; Passalacqua *et al*., 2010a; Orlandini *et al*., 2011; Jefferson and McGee, 2012). Whereas the threshold approaches were intended to predict the occurrence of channels based on coarse resolution DTMs under the assumption of landscape equilibrium (Montgomery and Foufoula-Georgiou, 1993), it also became evident that high-resolution DTMs are needed to detect geomorphic parameters related to channel heads and first-order streams in complex terrains (Tarolli and Dalla Fontana, 2009; Pirotti and Tarolli, 2010; Orlandini *et al*., 2011). Moreover, new extraction methods relying on high-resolution DTMs and computation of local topographic parameters are now available and able to suitably detect channel heads and channel networks (see Tarolli, 2014 for a review). In alpine terrains, Passalacqua *et al*. (2010a), Orlandini *et al*. (2011) and Henkle *et al*. (2011) outlined two main processes for channel initiation related to surface erosion/landsliding and lateral and upward groundwater seepage.

Several studies have also highlighted the importance of differentiating between perennial and intermittent networks, which yields seasonal fluctuations in drainage densities (Buttle *et al*., 2012; Godsey and Kirchner, 2014). In most hydrological models, the channel network is extracted from DTMs and compared with orthophotos or channel networks derived from official maps established by public agencies. However, a differentiation between intermittent and perennial streams is seldom noted because a field-mapping campaign would be required. All the aforementioned problems become more critical in high-mountain settings for a number of hydrologic processes and factors that are highly seasonal (Lehning *et al*., 2006; Simoni *et al*., 2011).

In this work, we investigate the ability of various automatic extraction methods to accurately capture the spatial variability of the channel network. In particular, we study the effect of using different channel networks, as well as the effect of differentiating between intermittent and perennial streams in the channel network, on the RWFs and on geomorphological characteristics in a high alpine headwater catchment. Although issues of nonstationarity and variance in the hydrologic response are currently the subject of much debate, especially with regard to source areas roughly identified here as unchannelled sites (McDonnell, 1990; Davies *et al*., 2013; McDonnell and Beven, 2014), and thus the utility of RWFs

are not universally agreed upon, we argue here that the RWF concept is useful in comparing the effects of a spatially heterogeneous channel network on key features of the catchment hydrologic response. The RWF concept is used here as a comparative tool to assess the accuracy of various extraction methods that are used to describe of the channelled portion of the watershed.

The manuscript is organized as follows: After a description of the study site, the available dataset and the mapping campaign are presented in Section on Study Area and Survey, the various extraction techniques and channel network comparison criteria are presented in Section on Methods and the results of the study are shown in Section on Results. After considering some implications and limits of our study in Section on Discussion, the conclusions are reported in Section on Conclusions.

STUDY AREA AND SURVEY

Field site

The Val Ferret watershed (Figure 1) is located in the Swiss Alps in the southernmost ridge that borders Italy. It covers a total surface of 20.4 km^2 with elevation ranges from 1773 m above sea level (a.s.l.) at the outlet of the catchment, to 3236 m a.s.l. (mean elevation: 2422.8 m a.s.l.). The catchment is studied in Simoni *et al.* (2011) and the watershed is described in detail there. The slopes are moderate to steep (mean slope: 31.6°, maximum: 88.9°), and the valley is mainly oriented southeast to northwest. Vegetation covers 60% of the area, consisting of mountain grassland (58%) and shrubs (2%); bare ground covers 37.4%, consisting of talus deposit (24.7%) and bedrock outcrops (12.7%). Shallow landslides are also present in the north region of the catchment (Figure 1). A small glacier (*glacier des Angroniettes*) covers 2% of the total area, and the remaining 0.4% is made up of three small lakes (*lacs de Fenêtre*) that feed the main river throughout the year. The climate of the study area is Alpine; snow covers the area from late fall until late spring.

This site has been monitored since 2008 with several gauging stations and a wireless network of small meteorological stations using Sensorscope technology (Ingelrest *et al.*, 2010). Apart from a water intake of maximum 171 per second and four cottages in the valley, the anthropogenic influence on the hydrological regime and the micrometeorological processes is minimal. This field site has been used to study the spatial variability of the main forcing on hydrological models (Simoni *et al.*, 2011), to develop new types of rating curves (Weijs *et al.*, 2013), to link streamflow recession flows to basin geomorphology (Mutzner *et al.*, 2013), to study katabatic and anabatic flows on steep slopes (Nadeau *et al.*, 2012; Oldroyd *et al.*, 2014) and to analyse controls on diurnal streamflow cycles (Mutzner *et al.*, 2015).

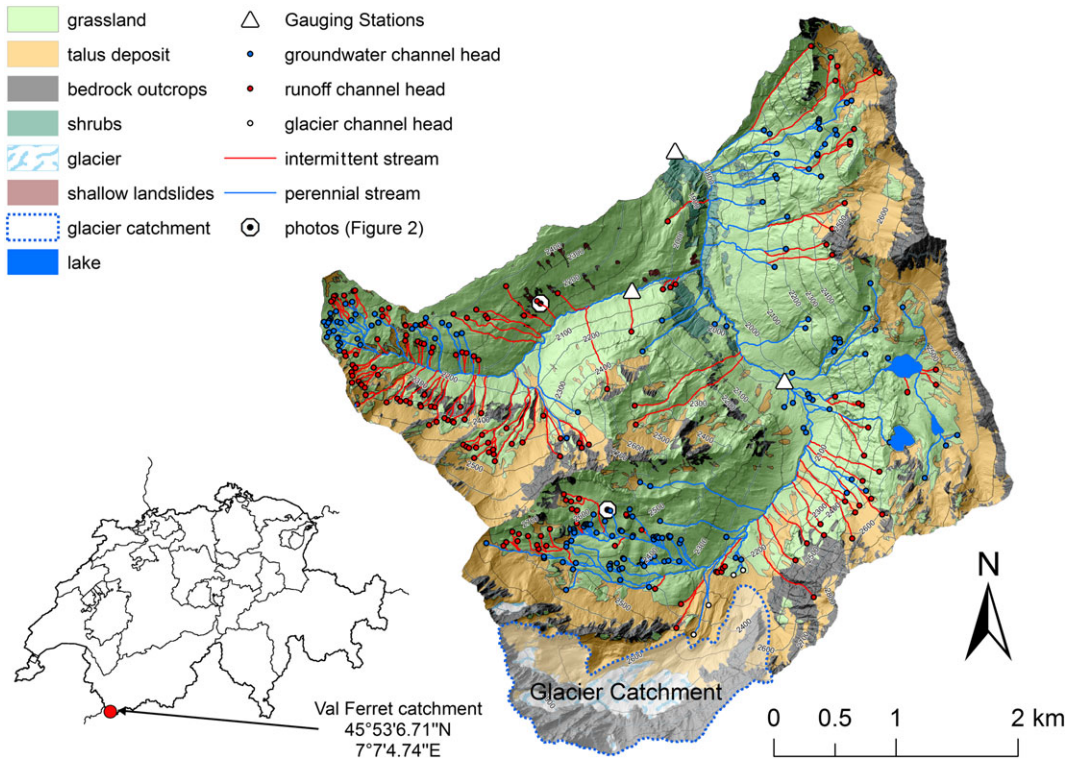

Figure 1. Topographic map of the study area. Channel heads and their type, channels and their state, gauging stations and land surface properties are shown in the map, along with the location of the photos shown in Figure 2

A 1-m resolution LiDAR-derived DTM was acquired in September 2010 by the company Helimap System SA. The survey point density was specified to 4–5 points per square metre, with absolute vertical and horizontal accuracy advertised by the company of respectively 10 and 15 cm in flat areas. Aerial 0.25-m resolution photographs were obtained from the Swiss Federal Office of Topography (see www.swisstopo.ch for more details).

Survey of the channel network and channel heads

In August 2011, an intensive field campaign was conducted in the Val Ferret watershed to map the channel heads and the channel network. At this time of the year, the main river was in its low flow regime, mainly fed by the release of groundwater and glacier melt. We systematically walked up all continuous drainage lines of the watershed using a high-precision Global Navigation Satellite System ((GNSS), Topcon GRS-1 based on global positioning system and GLObal Navigation Satellite System (GLONASS) horizontal accuracy of approximately half a metre) in order to locate and map 373 channel heads (Figure 2a). Similarly to Orlandini *et al.* (2011) and Passalacqua *et al.* (2010a), the positions of the channel heads were defined as the upstream limit of concentrated flow, where the hillslope converges to an observable drainage line and downstream flow path. Based on field observations, and according to Orlandini *et al.* (2011) and Passalacqua *et al.* (2010a), the channel heads were classified into two categories: (1) 190 groundwater channel heads due to lateral and upward groundwater seepage, driven by perennial flow (Figure 2a), and (2) 183 runoff channel heads initiated by soil erosion or landslide processes due to surface or fast sub-surface runoff, driven by ephemeral flow during rainfall or snowmelt-induced events (Figure 2b). Four additional channel heads were mapped in the southernmost part of the watershed; these are initiated by water coming out of the moraine fed by glacier melt and are indicated as glacier channel heads in Figure 1. Some channel heads that were inaccessible but nonetheless well defined as surface runoff channel heads were also mapped using a 1-m-resolution hillshade map and aerial photographs and verified with pictures taken in the field. Based on observations during the field survey, the channels were classified as perennial when there was water flowing in the transect and as intermittent when there was no water flowing (Figure 1). The bankfull width of the mapped channels ranged from 1–2 up to 15–20 m at the outlet. In the following, we refer to the channel network resulting from the survey as the *mapped network* and the wet part of this network as *perennial network*.

METHODS

Channel network extraction

Our study site is characterized by the presence of a small glacier in the southernmost part of the watershed (Figure 1). This area results in a complex morphology with pronounced surface concavities/convexities that are completely unrelated to the channel network. Therefore, we decided to mask these areas to prevent glacial channels from being erroneously considered as part of the river network. This area, depicted in Figure 1 as 'glacier catchment', represents 8.3% of the total watershed. In this work, we considered the following three different channel network extraction methods:

Area and slope-area threshold approaches. The area threshold and the slope-area threshold methods are widely used in the literature and are defined as 'classical approaches' for extracting the channel network. After removing depressions in the DTM, the flow direction is computed by following the steepest path among the neighbouring cells (d8 method, O'Callaghan and Mark, 1984). A concentrative method was used instead of a multiple flow direction method (Tarboton, 1997) to avoid

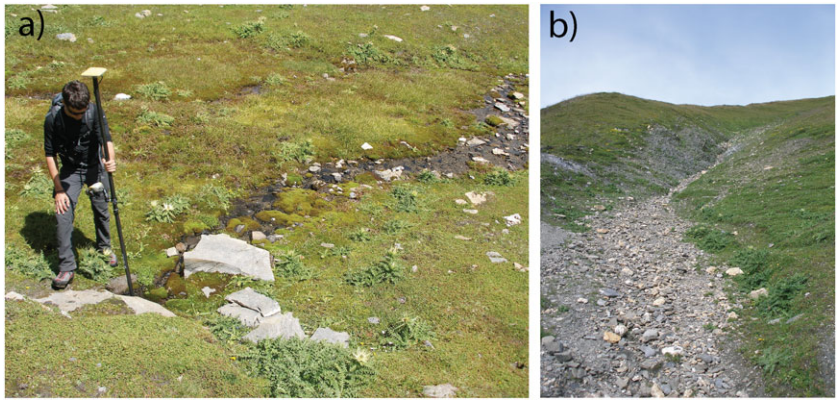

Figure 2. Examples of (a) a channel head formed by groundwater seeping upward flow in a low-slope area; (b) a channel head formed by a combination of flow accumulation and slope, with soil erosion in the Val Ferret experimental area

numerical dispersion of area from one cell to all neighbouring cells (Orlandini *et al*., 2003; Di Lazzaro, 2009). The contributing area and the local slope, which is defined per cell as the drop over distance ratio along the steepest descent, were computed for each of the channel heads mapped in the field. Averaged values of all channel heads were used to determine the drainage area threshold A_t and the slope-area threshold AS^k. We used the function AS^k with $k=2$ as suggested by Montgomery and Dietrich (1992). The network is then extracted by identifying cells with values larger than the aforementioned thresholds and by following the steepest path until the outlet is reached. The resulting channel networks will be referred to as *area threshold* and *slope area threshold*.

In addition, we also determined larger thresholds so that the resulting networks would have the same channel network length as the mapped network, i.e. the same Hortonian drainage density D_d, defined as the total length of stream channels divided by the area they occupy (Horton, 1932). These two resulting channel networks are referred as *area threshold 2* and *slope area threshold 2*.

Statistical approach. A statistical approach has also been applied to obtain automatic extraction of a channel network (Sofia *et al*., 2011). As this approach integrates both curvature (Evans, 1979) and topographic openness (Yokoyama *et al*., 2002), it is less affected by errors in the original topographic data. The openness, which is an angular measure of the relation between the surface morphology and horizontal distance, indeed avoids uncertainties related to the second derivative operation. This approach also provides a framework for an automatic definition of the optimum scale needed to analyse topographic attributes. Changing the size of the moving window manually, selecting windows that are too large or too small with respect to the correct one, could lead to biased results. However, Sofia *et al*. (2011, 2013, 2015) proved the robustness of the automatic methodology for different datasets in the absence of errors in the DTMs.

The core idea of the Sofia *et al*. (2011) methodology is to use statistical descriptors to objectively identify channels in which terrain geometry denotes a significantly convergent topography. Surface convergences are identified using two topographic attributes: minimum curvature (Evans, 1979) and openness (Yokoyama *et al*., 2002). The choice of the optimum scale of analysis (kernel) is automatic, and it relies on a statistical analysis of the topographic attribute distributions: The optimum kernel is the one that provides the greater asymmetry in the topographic parameter distribution (Sofia *et al*., 2011). In our study case, the kernel is found to be 15 m for openness and 11 m for curvature.

Once the kernel is identified, the network extraction procedure is then a three-step method based on (i) the normalization and overlapping of openness and minimum curvature in order to highlight the more likely surface convergences, (ii) a weighting of a multiple-flow upslope area (Quinn *et al*., 1991) according to such normalized maps to identify drainage flow paths and flow accumulation consistent with terrain geometry and (iii) the use of a value derived from the *z*-score normalization of the weighted upslope area as non-subjective threshold for channel network identification (Sofia *et al*., 2011). To obtain a fully connected network, a noise-filtering and connection procedure is applied to the potential extracted network (Sofia *et al*., 2011). Morphological methods based on curvature, in fact, can result in a skeleton network that appears disrupted. In Lashermes *et al*. (2007), the choice of which channels to trace is user dependent. In Passalacqua *et al*. (2010a,2010b), the introduction of a contributing area criterion eliminates all the isolated pixels with positive curvature above the threshold but that are not part of the channel network. In Sofia *et al*. (2011), false positives are discarded according to a majority filter: Cells belonging to the extraction are filtered based on the majority of their contiguous neighbouring cells. This filter requires neither any additional parameters nor *a priori* knowledge of the area. The basic idea is that thresholding extractions are typically characterized by fragmentation, and of these fragments, network fragments are fairly linear and regular, whereas noise is characterized by localized pixels or groups of pixels with a more rounded shape. Users can visually inspect the extraction map, and if localized nonlinear elements are present, apply the majority filter until they are discarded. The connection of the final network is then based on a shortest cost path approach, where the cost of travelling from one cell to the other is given by the Euclidean distance of that cell from the extracted network (Sofia *et al*., 2011). The resulting channel network extracted with this method will be referred as the s*tatistical approach*.

Geomorphological characterization of the channel network

We use several geomorphological descriptors to compare the channel networks obtained with the different extraction methods: (1) the Hortonian drainage density D_d, expressed in km/km^2, (2) the watershed order Ω, (3) the drainage frequency expressed in number of streams per unit of area (#/km^2) and (4) the distance from the farthest channel head to the outlet along the network (metre). These parameters, sensitive to the extraction method, are often used to compare basins of different size or to establish catchment-scale hydrological parameters.

We also compute the local hillslope-to-channel distance L_h, defined per cell as the length covered following the steepest descent path among the eight neighbouring cells until a channelized cell is reached. The classical

Hortonian drainage density D_d is approximately taken as the inverse of two times the mean hillslope-to-channel distance (Horton, 1945). Hence, the hillslope-to-channel distance L_h can be seen as a local measure of the drainage density (Tucker *et al*., 2001). As proposed in Tucker *et al*. (2001), the hillslope-to-channel distance L_h is treated as a spatial random function allowing one to compute the probability distribution function and covariance function of L_h. It is expected, as in Rinaldo *et al*. (1995), that the length distribution calculated in this manner, at least in shallow soils punctuated by bedrock emergence and topographic complexity, is an essential ingredient for determining the ensemble mean hydrologic response. The covariance function, computed under the assumption of isotropy and second-order stationarity (Tucker *et al*., 2001), is fitted with an exponential model with an effective range, a widely accepted model in geostatistics (Goovaerts, 1997). The computation of this effective range is used to find a suitable scale to use to map drainage density at the sub-catchment scale.

Width function and rescaled width function

The width function is computed as the number of cells located at a given distance from the outlet following the river network, normalized by the total number of cells belonging to the channel network. When the hillslope's contribution to total travel length is taken into effect in the calculation, we can compute the RWF defined as follows (Rinaldo *et al*., 1995; Grimaldi *et al*., 2010):

$$\tau(x,y) = \frac{L_h(x,y)}{u_h} + \frac{L_c(x,y)}{u_c} \quad (1)$$

where τ is a theoretical lag time from every cell to the outlet, L_c is the flow path across the channels and L_h is the hillslope-to-channel distance. The parameters u_h and u_c are the hillslope and channel celerity, respectively, that control the propagation of a pressure wave and that are not to be confused with water velocities that control water transport (McDonnell and Beven, 2014). The RWF, corresponding to a catchment's geomorphological instantaneous unit hydrograph, is then obtained by normalizing the lag time τ of each cell by the total number of cells, i.e. the catchment area. This lag time does not describe flow or transport travel times, the ones involved in runoff generation, also driven by celerity, nor solute transport, driven by advective velocities but rather describes the geomorphic effect on the hydrologic response through the RWF.

The computation of the RWF requires the estimation of the two parameters u_h and u_c. In our study, we decided to use a constant channel celerity of 2 m/s and to compute the RWF for three different cases of hillslope celerity, namely, $u_h = 0.04$ m/s, $u_h = 0.2$ m/s and $u_h = 0.1$ m/s. Effects of major variations in the ratio u_h/u_c have been dealt with elsewhere (Rinaldo *et al*., 1995; Botter and Rinaldo, 2003; D'Odorico and Rigon, 2003). Our purpose here is comparative, i.e. to test whether the extracted channel networks are able to reproduce the RWF when taking the mapped network as a reference, and the particular choice of the parameters u_h and u_c does not affect our conclusions. The choice of the channel celerity value of 2 m/s was motivated by observation of glacier melt-induced streamflow diurnal cycles at the outlet of a sub-catchment and at the outlet of the watershed (Simoni *et al*., 2011; Mutzner *et al*., 2015). The channel celerity, computed as the time difference in the occurrence of maximum streamflow divided by the distance between the two outlets along the channel network, was found to be relatively constant at values oscillating between 1.5 and 2.5 m/s. The choice of different hillslope celerities will be discussed later, but the three hillslope celerities used in our study are comparable with values used in other RWF-based studies. Note that the hillslope celerities were considered uniform across the basins so that variability of the hillslope celerity within the catchment was not taken into account. This will be discussed in a later section.

RESULTS

Location and characterization of channel heads

The mean, median and standard deviation of the drainage area and local slope of the mapped channel heads are shown in Table I. A box plot of drainage area and local slope for both channel head types is shown in Figure 3. The groundwater channel heads tend to present a lower critical support area and lower slope compared with the runoff

Table I. Statistical characteristics of drainage area and local slope of the mapped channel heads with and without classification. The term *std* stands for standard deviation

	Area (m^2)			Slope ($m\,m^{-1}$)		
	Mean	Median	std	Mean	Median	std
All channel heads	6092	1296	17649	0.447	0.411	0.275
Groundwater	2879	895	6801	0.407	0.361	0.273
Runoff	8983	2246	23863	0.488	0.484	0.272

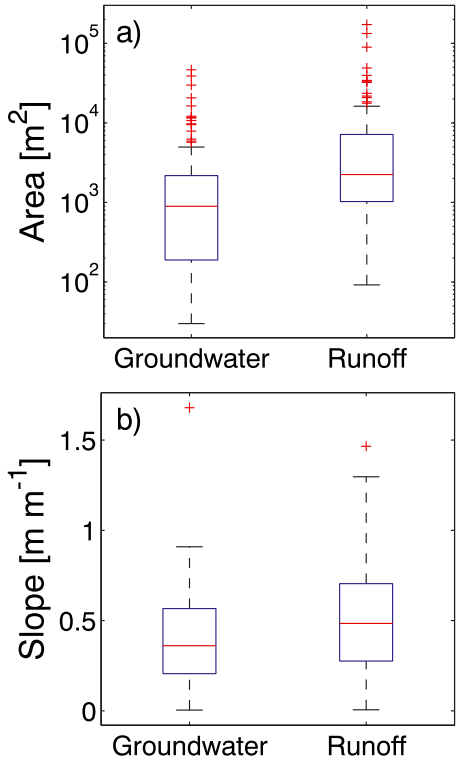

Figure 3. Box plots of contributing area and local slope for each channel head types

channel heads. Moreover, the standard deviation of the local drainage area is much larger than the mean, indicating a large spatial variability in the channel initiations.

We performed a non-parametric Mann–Whitney U test at a level of significance $\alpha = 0.05$ to test the null hypothesis that groundwater and runoff channel heads have identical continuous distributions of drainage area and local slope. In the channel head drainage areas, we found a small p-value ($1.24 \cdot 10^{-13}$) suggesting a highly statistically significant difference between groundwater and runoff channels. In the case of the local slope, the p-value was larger (0.003) but still indicates that the distribution of the slope of the two channel head groups is different. This simply suggests that the contributing area is a better descriptor than local slope for separating groundwater channel heads from runoff channel heads. A power law was fitted through least squares between the contributing area and the local slope, but the correlation was found to be weak for each channel head type ($R^2 = 0.0044$ for groundwater channel heads and $R^2 = 0.031$ for runoff channel heads).

Channel network characterization

Thresholds of 6092 and 1675 m^2 were respectively used to extract the channel networks' *area threshold* and *slope area threshold*. These thresholds correspond to an average of all the mapped channel heads without distinction (Table I) and are also referred as field-based thresholds. For the channel networks *area threshold 2* and *slope area threshold 2*, values of 21959 and 25475 m^2 were used as thresholds to obtain the same Hortonian drainage density as the mapped network. Table II summarizes some geomorphological parameters of the extracted networks. As expected, all the parameters change with the differently extracted channel networks. The difference in Hortonian drainage density obtained with the classical methods and field-based thresholds is particularly large. Between the two classical methods, the discrepancy is the largest for the slope-area method. Even though the watershed order obtained with the statistical approach is not correct, the drainage density and drainage frequency are close to those obtained with the mapped network. We also note that the area and slope-area methods appear to do satisfactorily when used with a larger threshold (*area threshold 2* and *slope area threshold 2*). In particular, the drainage frequency is relatively close to that obtained with the mapped network. Finally, we note that the distance from the farthest channel head to the outlet is similar in the different channel networks, although the *area threshold 2* and the *slope area threshold 2* networks tend to underestimate it. For the mapped network, we found that over the total channel network length, 52.9% of the channels are perennial and the remaining 47.1% are intermittent channels activated during rainfall or snowmelt events. The Hortonian drainage density and the drainage frequency of the perennial network therefore make up almost half of the mapped network.

Table II. Geomorphological features of the extracted networks

Extraction method	Drainage density D_d (km/km^2)	Watershed order Ω	Drainage frequency (#/km^2)	Longest distance to outlet (m)
Mapped network	5.27	6	32.99	8046.12
Statistical approach	4.82	5	33.97	8002.32
Area threshold	11.50	6	92.45	8291.07
Slope area threshold	27.18	7	457.06	8348.38
Area threshold 2	5.27	5	26.27	8207.21
Slope area threshold 2	5.27	5	26.23	8013.11
Perennial network	2.79	5	16.27	8046.12

The width function obtained with the various networks is shown in Figure 4. We note some common features, although significant differences can be observed between the different extraction methods. For example, except for the perennial network, the dominant flow distance (roughly located between 0.5 and 0.65) is well captured by all the extraction methods. This is due to the fact that the highest-order channels are well identified by all the methods. When considering only the classical methods, the discrepancy is the largest for normalized flow distances between 0.3 and 0.4. The discrepancy is also important for all methods at large flow distances, i.e. for the low-order streams with some peaks of the mapped network width function that none of the channel network extraction methods is able to capture.

Study of the hillslope-to-channel distance

Figure 5 shows both the extracted channel networks in blue and the colour-coded hillslope-to-channel distance L_h obtained in the case of the different channel networks. For clarity, the results obtained with the perennial network are not shown in Figure 5. As can be seen in panel (a), the mapped channel network is characterized by a local drainage density that is spatially heterogeneous. In particular, we observe a high density of channels in the westernmost and southwesternmost parts of the catchment resulting in low values of L_h. On the contrary, we observe a very low density of channels relatively close to the outlet and close to the glacier catchment that none of the classical methods is able to capture. The classical methods with low field-based threshold values (*c* and *d*) clearly exhibit a much larger extent of channelled portions of the landscape than indicated by the mapped network. When used with larger threshold values (*e* and *f*, same Hortonian drainage density as the mapped network), the classical extraction methods present a better match in spatial distribution of the hillslope-to-channel distance L_h. However, with this larger threshold value, the two classical methods are not able to capture the high density of channels observed in the westernmost and southwesternmost parts of the catchment. We note from Figure 5 that the hillslope-to-channel distance L_h tends to be larger in the areas covered by bedrock emergences, such as in the easternmost part of the catchment.

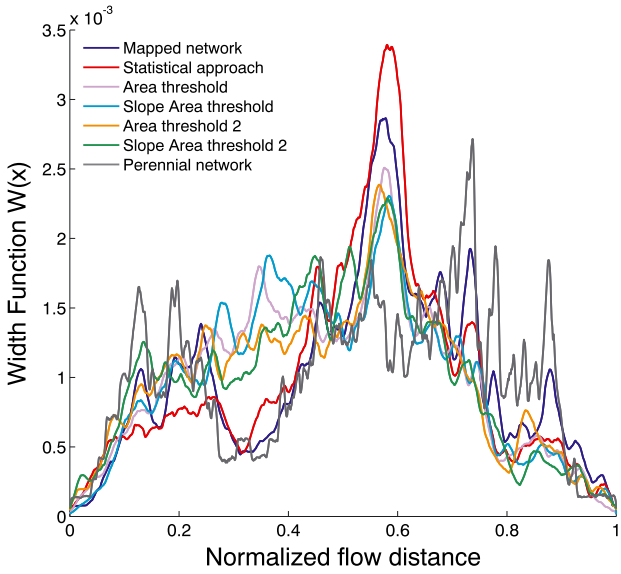

Figure 4. Width function of the watershed using the different network extraction methods

As previously mentioned, L_h is treated as a random function, allowing the computation of a probability distribution as in Tucker *et al.* (2001), which is presented in Figure 6 for the different channel networks. The distances have been normalized by the largest hillslope-to-channel distance found for the mapped network ($L_{h,max} = 1529.9$ m, note that the maximum distance L_h of 2470.2 m mentioned in Figure 6 is to be found in the glacier catchment that has been discarded in our calculations, see section on Methods). The mean, maximum and standard deviations for the different extraction methods are listed in Table III. When used with the lower field-based thresholds, the classical methods completely underestimate the hillslope-to-channel distance, leading to a severe overestimation of the Hortonian drainage density. This is especially the case for the slope-area method with a mean hillslope-to-channel distance of 63.6 m, more than four times smaller than the value found with the mapped network. The maximum hillslope-to-channel distance is also greatly underestimated with the classical network methods. When used with larger threshold values, the classical methods also tend to underestimate the hillslope-to-channel distance L_h. Interestingly, the slope-area method is closer to the mapped network than the area method when used with a larger threshold value. The discrepancy between the statistical approach and the mapped network is smaller, although the statistical approach tends to overestimate the hillslope-to-channel distance. The discrepancy is also relatively large when only the perennial channels of the network are considered. Indeed, the hillslope-to-channel distance tends to be larger when the intermittent channels are not considered, leading to an increase in the mean and maximum hillslope-to-channel distance of, respectively, 56.3% and 27.9%.

The covariance functions of L_h are presented in Figure 7. As expected, L_h is strongly autocorrelated at the scale of individual hillslopes (short lag distance *r*). At larger scales, the covariance breaks down to values oscillating around zero. The covariance of the different networks has been computed for maximum radial distances of 1600 m. Note that the covariance of the perennial network also oscillates around zero, but for

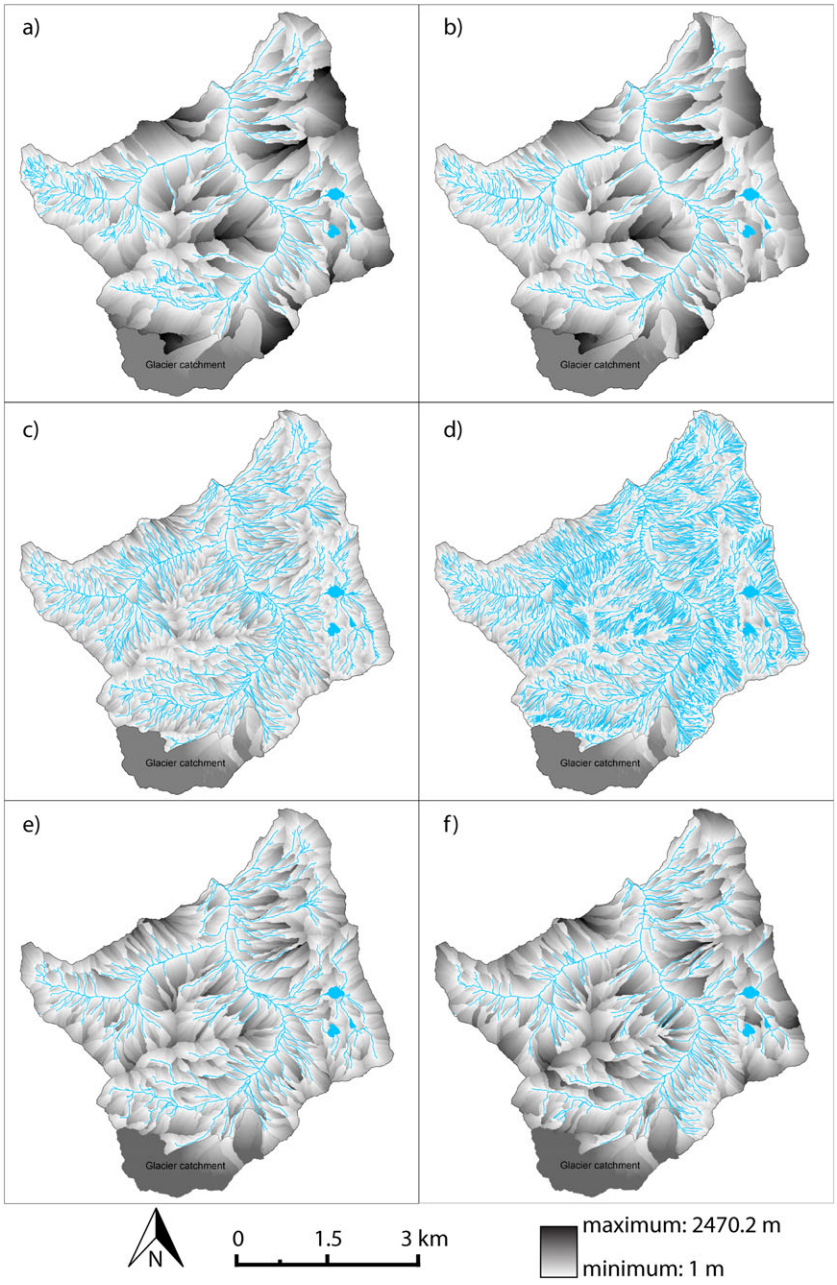

Figure 5. Hillslope-to-channel distance L_h and channel network for different methods: (a) mapped network, (b) the statistical approach, (c) the area method with field-based threshold, (d) the slope-area method with field-based threshold, (e) the area method with larger threshold and (f) the slope-area method with larger threshold

larger lags, which for purposes of clarity are not shown in Figure 7. The covariance function of the statistical approach is close to that of the mapped network, whereas the correlation breaks down faster with the classical methods and more slowly for the perennial network. An exponential model with an effective range has been fitted to all the computed covariance functions of Figure 7; the values of the effective range can be found in Table III along with the coefficient of determination. The results show again that the statistical approach agrees better with the mapped network results than the classical network approaches. Even though the results improve when we use a larger value of the threshold for the classical methods (*area threshold 2* and *slope area threshold 2*), the effective range is still approximately half the value of that found in the mapped network. Among the two classical methods used with larger threshold values, the covariance of the slope-area method (*slope area threshold 2*) is closer to the mapped network than the area method. In the case of the perennial network, the effective range increases

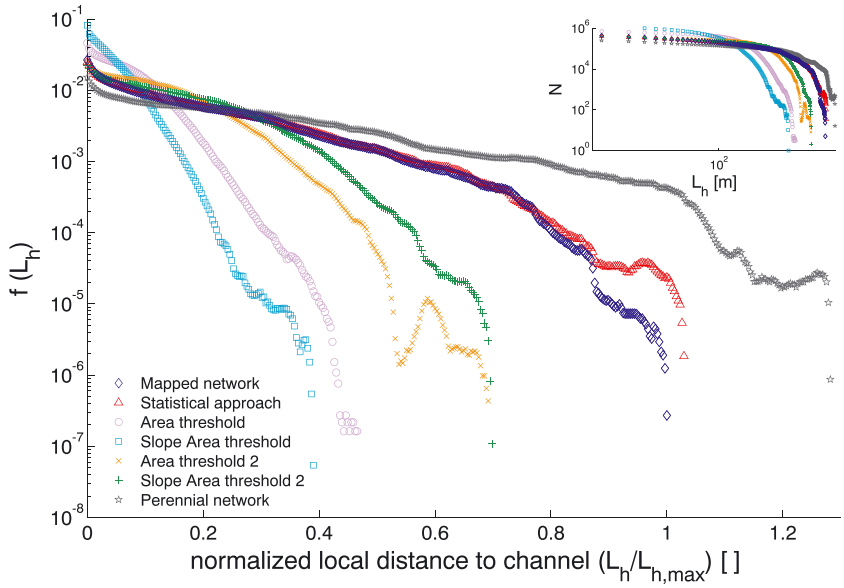

Figure 6. Frequency distribution of the hillslope-to-channel distance L_h for the different extraction methods. The local distance to channel has been normalized by the maximum value of L_h ($L_{h,max}$ = 1530 m) computed with the mapped network. Upper right plot: frequency distribution of L_h without normalization

Table III. Properties of the hillslope-to-channel distance obtained with the different extracted networks

Extraction method	$L_{h,mean}$ (m)	σ_L (m)	$L_{h,max}$ (m)	Effective range (m)	R^2
Mapped network	280.66	256.31	1529.91	645.39	0.9696
Statistical approach	284.82	261.96	1574.52	674.1	0.9403
Area threshold	100.89	81.65	713.04	243.69	0.9646
Slope area threshold	63.60	57.29	595.3	124.75	0.9719
Area threshold 2	179.76	138.41	1058.93	330.13	0.9555
Slope area threshold 2	219.07	170.95	1066.55	395.27	0.9575
Perennial network	438.81	366.74	1957.76	791.02	0.9597

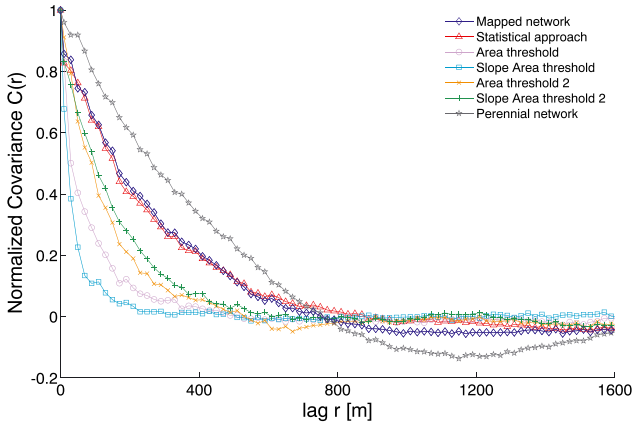

Figure 7. Covariance functions of the hillslope-to-channel distance L_h for the different channel network extraction methods. The values have been normalized by the variance of the hillslope-to-channel distance L_h for each method

by 22.5% compared with the mapped network. As proposed by Tucker *et al.* (2001) and based on our results obtained with the mapped network, the hillslope-to-channel distance could be averaged spatially by using a circular moving window of 645 m. This method allows the spatial variability of the drainage density to be quantified.

Comparative analysis of RWFs

The RWFs are presented in Figure 8 for three different cases of hillslope celerity. Their first three statistical moments along with the estimated time to peak and coefficient of determination are summarized in Table IV. As expected, the mean and standard deviation of the RWFs increase with decreasing hillslope celerity. For the mapped network, the estimated time to peak of the distribution is a relatively constant 50 min for all the three cases. All the channel networks are able to represent the estimated time to peak satisfactorily when compared with the mapped network, with small relative errors ranging from 7.5% for the *area threshold* network up to 13.5% for the *slope area threshold 2* network. We also observe that the amplitude of the RWF maximum decreases with decreasing hillslope celerity (Figure 8).

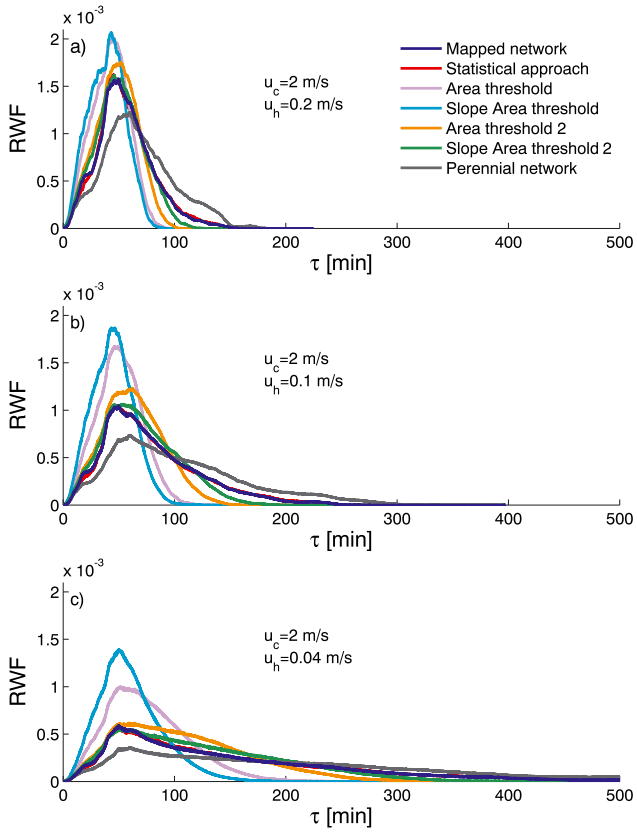

Figure 8. Rescaled width functions (RWFs) of the watershed using the different channel network extraction methods and different hillslope celerities. The legend in (b) and (c) is the same as in (a). For clarity, the RWFs in (c) have been truncated at 500 min

As expected (Rinaldo *et al.*, 1995), the RWFs become skewed positively with decreasing hillslope celerity (Table IV). Achieving a positive skewness is necessary to reproduce real recession events using the RWF approach. In the first case, where the channel and hillslope celerity are only separated by an order of magnitude, the skewness of the RWFs obtained with the mapped network, perennial and statistical approach networks is small (0.65, 0.66 and 0.54, respectively) and almost not skewed in the case of the classical approaches (−0.01, 0.04, −0.02 and 0.22). The skewness of the RWFs increases with decreasing hillslope celerity for all the networks. In the three different cases, the RWF of the statistical approach is similar to that obtained with the mapped network (average R^2 of 0.998). The discrepancy between the classical approaches distributions and the mapped network distribution is larger when the lower field-based thresholds are used (average R^2 of 0.418 and 0.008 for the *area threshold* and *slope area threshold* networks, respectively). However, as can be seen in Figure 8 and Table IV, the difference between the classical approaches and the mapped network is smaller when a larger threshold is used (average R^2 of 0.872 and 0.967 for the *area threshold 2* and *slope area*

Table IV. Moments of the rescaled width function for the three different cases of hillslope celerities. The units of the mean, the standard deviation (STD) and estimated time to peak (t_{max}) are expressed in minutes, whereas the skewness (SKW) and coefficient of determination R^2 are unitless. The mapped network was taken as a reference for computing the coefficient of determination

	Case 1 $u_c = 2$ m/s $u_h = 0.2$ m/s					Case 2 $u_c = 2$ m/s $u_h = 0.1$ m/s					Case 3 $u_c = 2$ m/s $u_h = 0.4$ m/s				
Extraction method	t_{max}	Mean	STD	SKW	R^2	t_{max}	Mean	STD	SKW	R^2	t_{max}	Mean	STD	SKW	R^2
Mapped network	49.92	56.01	24.66	0.65	—	49.83	79.43	43.61	1.02	—	50.25	149.68	106.08	1.17	—
Statistical approach	45.33	56.30	24.77	0.66	0.997	45.17	80.03	44.17	1.05	0.999	50.25	151.14	107.86	1.20	0.998
Area network	46.17	42.52	16.21	−0.01	0.691	46.17	50.92	19.83	0.19	0.397	51.08	76.15	36.61	0.77	0.165
Slope area network	43.17	39.72	15.84	0.04	0.529	46.50	45.02	17.97	0.22	0.005	50.33	60.92	28.52	0.87	−0.509
Area network 2	51.83	48.43	18.24	−0.02	0.920	62.00	63.41	26.56	0.32	0.862	64.58	108.35	58.49	0.75	0.835
Slope area network 2	46.17	51.38	20.91	0.22	0.980	54.00	69.64	32.54	0.52	0.968	59	124.40	73.20	0.76	0.953
Perennial network	60.17	67.85	31.18	0.54	0.865	60.33	104.42	59.82	0.86	0.849	60.17	214.12	150.34	0.99	0.838

threshold 2 networks, respectively). In particular, the RWF of the *slope area threshold 2* is closer to the mapped network than that obtained with *area threshold 2*. For the perennial network, the discrepancy with the mapped network is large and similar in all three cases of hillslope celerity (average R^2 of 0.851).

DISCUSSION

As illustrated in Figure 2, some low-order channels have a bankfull width that is in the same order of magnitude as the DTM resolution. Using DTMs of coarser resolution would result in an underestimation of the drainage frequency and the drainage density, because some channel heads that are separated by only a few metres would be unresolved, and the low-order channels would not be captured by the coarse pixel size. This is in agreement with Tarolli and Dalla Fontana (2009), who showed that when dealing with detection of channel heads based on statistic thresholds of topographic parameters, finer resolutions were indeed more reliable.

We note that groundwater channel heads occur at lower total contributing drainage area when compared with ephemeral runoff-controlled channel heads, confirming that the initiation processes are of different nature, in agreement with previous findings in alpine contexts (Passalacqua *et al*., 2010a; Henkle *et al*., 2011; Orlandini *et al*., 2011). Groundwater channel heads present lower values of local slope with respect to runoff channel heads, but the local slope is a less powerful criterion to differentiate the two groups of channel heads. High-altitude environments present a complex scenario in which different channel initiation processes coexist and where exposed lithology and shallow soil profiles are reflected by very heterogeneous drainage density. This is partly driven by groundwater seepage and saturation from below and partly by other processes unrelated to contributing area and local slope (e.g. precipitation, snowmelt events or vertical cliff erosion in hollows). Given the high variability of contributing area and local slope of the channel heads, our results also confirm earlier findings that a unique threshold for channel head identification might not exist at the catchment scale (Jaeger *et al*., 2007; Tarolli and Dalla Fontana, 2009; Passalacqua *et al*., 2010a; Orlandini *et al*., 2011; Jefferson and McGee, 2012).

The drainage density was found to be quite heterogeneous at the catchment scale. In particular, we observed a high density of streams in the parts of the catchment where a high density of groundwater channel heads was surveyed and lower channel density where runoff channel heads were mapped. Even though we used averaged values of the mapped channel as thresholds (i.e. field-based thresholds), the classical extraction methods severely overestimated the drainage density of the watershed. To obtain a drainage density equal to that of the mapped network, the thresholds chosen had to be much larger than the average of the mapped channel heads. These higher thresholds are not representative of the different channel head initiation processes, however, thus exemplifying the problem inherent to choosing a unique threshold for channel initiation.

The spatial variability of the drainage density was also illustrated by large variations of the hillslope-to-channel distance. The autocorrelation scale of the hillslope-to-channel distance was much smaller than the catchment width, illustrating that drainage density is highly uneven in this mountainous environment. When classical methods were used with larger thresholds, the results obtained with the *slope area threshold 2* network were better than the ones obtained with the *area threshold 2* network (Table III and Figures 6 and 7). This is due to the ability of the slope-area method to account for uneven drainage densities. However, even though the Hortonian drainage densities of the *area threshold 2* and *slope area threshold 2* networks were equal to the drainage density obtained with the mapped network, large discrepancies were observed in the frequency distribution and the covariance function of the hillslope-to-channel distance using these methods. This shows that none of the classical methods is able to accurately capture the spatial variability of the drainage density and highlights some limits of the classical definition of the Hortonian drainage density. Indeed, the classical definition of the Hortonian drainage density is a good descriptor of how dissected a landscape is by channels, but does not reflect the marked heterogeneity in the spatial distribution of channels observed in mountainous regions. This had already been noted by Marani *et al*. (2003), who observed major differences between Hortonian and actual drainage densities in tidal environments in the northern lagoon of Venice. We therefore support the approach of Tucker *et al*. (2001) in adopting the framework that describes drainage density through the features of the probability distribution of unchannelled lengths.

The analysis of the RWFs showed that the results are sensitive to the channel network extraction methods. The different channel networks used in this study are able to reproduce the estimated time to peak satisfactorily with little differences in the occurrence of the distribution maximum. However, larger discrepancies were observed for longer lag times (Table IV). Indeed, the classical extraction methods tend to underestimate the hillslope-to-channel distances compared with those obtained with the mapped network and the statistical approach. Whereas classical methods were intended to predict the occurrence of channels when only coarse DTMs were available, the

statistical approach and other new methods based on high-resolution DTMs, such as the statistical approach used in this study, allow to detect topographic signatures of channel. Moreover, the classical methods are valid under the assumption of landscape equilibrium, which is not the case in alpine terrains such as the Val Ferret. It is therefore certainly not surprising that the statistical approach outperforms the classical approaches when the RWFs and the other descriptors used in this study are compared with the ones obtained with the mapped network. However, the classical methods remain by far the most widely used methods in the scientific community. Our results show that more advanced techniques should be used in complex environments, if a high-resolution DTM is available, given that the partitioning of the landscape into hillslope and channel network could affect the hydrological modelling as exemplified here within the RWF formalism.

It is also important to mention that hydrodynamic dispersion in the channels has not been taken into account in the calculation of the RWFs. However, a large positive skewness is already achieved when the hillslope and channel celerities are separated by two orders of magnitude. We acknowledge that our approach of using spatially constant hillslope and channel celerities is simplistic. It is known that hillslope celerities are state dependent (say, on soil moisture deficits) and vary both in space and time (McDonnell and Beven, 2014). However, our goal is not to discuss the validity of RWF-based models that account for spatially varying celerities (Grimaldi *et al*., 2010; Grimaldi *et al*., 2012; Petroselli, 2012) but rather to focus on the effect of the spatially heterogeneous channel network on RWFs, which are in turn seen as surrogates of expected features of the hydrologic response.

We argue that taking into account the state of the channels (intermittent or perennial) could play an important role in modelling real hydrographs in the RWF formalism. Even though the peak of the RWF was well captured when only the perennial network was used, the difference was larger for the decreasing part of the RWF. However, unless field-mapping campaigns are undertaken, it is a difficult task to identify the perennial part of the channel network based solely on remote sensing techniques. In addition, errors might be introduced in field-mapping campaigns when separating perennial streams from intermittent streams; some channels drying out late in the season might be incorrectly labelled as perennial channels. In our case, this error is unlikely because the mapping campaign was undertaken during low-flow conditions. To provide a realistic perennial network to use as reference, it is therefore important to carry out field mapping campaigns of channel heads and channels when the river is in its low-flow regime. Moreover, further research is needed to understand and model the possible ephemeral character of the active drainage network which in high mountain catchments can be conceptually linked to a seasonal evolution induced, for instance, by snowmelt in snow-covered catchment.

CONCLUSIONS

The accurate representation of stream networks is of fundamental importance in many hydrological and geomorphological applications. In this work, we studied the influence of spatially heterogeneous drainage densities on common geomorphological parameters, hillslope-to-channel distance and RWFs. The channel network and the channel heads were carefully mapped in the field using a high-precision GNSS device. We compared the mapped channel network with different channel networks obtained with (1) a statistical approach that considers statistical analysis of surface morphology and topographic parameters such as curvature and openness and (2) classical approaches using thresholds related to cumulative drainage area and local slope. Unlike the statistical approach, the classical methods were not able to reproduce the spatial variability of the drainage density nor the distribution of the hillslope-to-channel distance distribution and RWFs. Our results suggest that inaccurate channel delineation in high mountain catchments might affect the accuracy in models of the receding part of the storm hydrograph. For mountainous environments, we therefore recommend avoiding standardized channel network extraction criteria and suggest using techniques that rely on the analysis of surface morphology via high-resolution DTMs.

ACKNOWLEDGEMENTS

The authors are grateful to the Swiss National Science Foundation for its financial support (grant number 200021_134982/1 and 200021_153615) and to the NCCR-MICS, CCES and NSERC Discovery Grant funding. The authors thank the Commune d'Orsières for providing logistic support for the field campaigns. The DTM and the location of the channel heads are available upon request to Marc Parlange (marc.parlange@ubc.ca). The authors thank three anonymous reviewers, who provided very detailed comments that improved the paper.

REFERENCES

Beven K. 2011. *Rainfall–Runoff Modelling: The Primer*, 2nd edition. Wiley-Blackwell: Chichester, UK.

Borga M, Boscolo P, Zanon F, Sangati M. 2007. Hydrometeorological analysis of the 29 August 2003 flash flood in the Eastern Italian Alps. *Journal of Hydrometeorology* **8**: 1049–1067. DOI:10.1175/JHM593.1.

Botter G, Rinaldo A. 2003. Scale effect on geomorphologic and kinematic dispersion. *Water Resources Research* **39**(10). DOI:10.1029/2003WR002154.

Buttle J, Boon S, Peters D, Spence C, (Ilja) van Meerveld HJ, Whitfield P. 2012. An overview of temporary stream hydrology in Canada.

Canadian Water Resources Journal / Revue canadienne des ressources hydriques **37**: 279–310. DOI:10.4296/cwrj2011-903.

Cavalli M, Trevisani S, Comiti F, Marchi L. 2013. Geomorphometric assessment of spatial sediment connectivity in small Alpine catchments. *Geomorphology* **188**: 31–41. DOI:10.1016/j.geomorph.2012.05.007.

Comola F, Schaefli B, Rinaldo A, Lehning M. 2015. Thermodynamics in the hydrologic response: travel time formulation and application to Alpine catchments. *Water Resources Research* **51**. DOI:10.1002/2014WR016228.

Davies J, Beven K, Rodhe A, Nyberg L, Bishop K. 2013. Integrated modeling of flow and residence times at the catchment scale with multiple interacting pathways. *Water Resources Research* **49**(8): 4738–4750. DOI:10.1002/wrcr.20377.

Di Lazzaro M. 2009. Regional analysis of storm hydrographs in the rescaled width function framework. *Journal of Hydrology* **373**: 352–365. DOI:10.1016/j.jhydrol.2009.04.027.

Di Lazzaro M, Volpi E. 2011. Effects of hillslope dynamics and network geometry on the scaling properties of the hydrologic response. *Advances in Water Resources* **34**: 1496–1507. DOI:10.1016/j.advwatres.2011.07.012.

D'Odorico P, Rigon R. 2003. Hillslope and channel contributions to the hydrologic response. *Water Resources Research* **39**. DOI:10.1029/2002WR001708.

Evans IS. 1979. An integrated system of terrain analysis and slope mapping. Final report on grant DA-ERO-591-73-G0040, University of Durham: England.

Gandolfi C, Bischetti GB. 1997. Influence of the drainage network identification method on geomorphological properties and hydrological response. *Hydrological Processes* **11**: 353–375.

Giannoni F, Smith JA, Zhang Y, Roth G. 2003. Hydrologic modeling of extreme floods using radar rainfall estimates. *Advances in Water Resources* **26**: 195–203. DOI:10.1016/S0309-1708(02)00091-X.

Giannoni F, Roth G, Rudari R. 2005. A procedure for drainage network identification from geomorphology and its application to the prediction of the hydrologic response. *Advances in Water Resources* **28**: 567–581. DOI:10.1016/j.advwatres.2004.11.013.

Godsey SE, Kirchner J. 2014. Dynamic, discontinuous stream networks: hydrologically driven variations in active drainage density, flowing channels, and stream order. *Hydrological Processes* **28**: 5791–5803. DOI:10.1002/hyp.10310.

Goovaerts P. 1997. *Geostatistics for Natural Resources Evaluation*. Oxford University Press: New York, NY.

Grimaldi S, Petroselli A, Alonso G, Nardi F. 2010. Flow time estimation with spatially variable hillslope velocity in ungauged basins. *Advances in Water Resources* **33**: 1216–1223. DOI:10.1016/j.advwatres.2010.06.003.

Grimaldi S, Petroselli A, Nardi F. 2012. A parsimonious geomorphological unit hydrograph for rainfall–runoff modelling in small ungauged basins. *Hydrological Sciences Journal* **57**: 73–83. DOI:10.1016/j.advwatres.2010.06.003.

Gupta VK, Mesa OJ. 1988. Runoff generation and hydrologic response via channel network geomorphology – recent progress and open problems. *Journal of Hydrology* **102**: 3–28. DOI:10.1029/WR016i005p00855.

Henkle JE, Wohl E, Beckman N. 2011. Locations of channel heads in the semiarid Colorado Front Range. *Geomorphology* **129**(3–4): 309–319. DOI:10.1016/j.geomorph.2011.02.026.

Horton RE. 1932. Drainage basin characteristics. *Transactions of the American Geophysical Union* **13**: 348–352.

Horton RE. 1945. Erosional development of streams and their drainage basins; hydrophysical approach to quantitative morphology. *Geological Society of America Bulletin* **56**: 275–370.

Ingelrest F, Barrenetxea G, Schaefer G, Vetterli M, Couach O, Parlange MB. 2010. SensorScope: application-specific sensor network for environmental monitoring. *ACM Trans. Sen. Netw.* **6**(2): 1–32. DOI:10.1145/1689239.1689247.

Jaboyedoff M, Oppikofer T, Abellán A, Derron MH, Loye A, Metzger R, Pedrazzini A. 2012. Use of LIDAR in landslide investigations: a review. *Natural Hazards* **61**: 5–28. DOI:10.1007/s11069-010-9634-2.

Jaeger K, Montgomery D, Bolton S. 2007. Channel and perennial flow initiation in headwater streams: management implications of variability in source-area size. *Environmental Management* **40**(5): 775–786. DOI:10.1007/s00267-005-0311-2.

Jefferson AJ, McGee RW. 2012. Channel network extent in the context of historical land use, flow generation processes, and landscape evolution in the North Carolina Piedmont. *Earth Surface Processes and Landforms* **38**: 601–613. DOI:10.1002/esp.3308.

Kirkby MJ. 1976. Tests of the random network model, and its application to basin hydrology. *Earth Surface Processes* **1**: 197–212. DOI:10.1002/esp.3290010302.

Lashermes B, Foufoula-Georgiou E, Dietrich WE. 2007. Channel network extraction from high resolution topography using wavelets. *Geophysical Research Letters* **34**. DOI:10.1029/2007GL031140.

Lehning M, Vöksch I, Gustafsson D, Nguyen TA, Stähli M, Zappa M. 2006. ALPINE3D: a detailed model of mountain surface processes and its application to snow hydrology. *Hydrological Processes* **20**: 2111–2128. DOI:10.1002/hyp.6204.

Marani M, Belluco E, D'Alpaos A, Defina A, Lanzoni S, Rinaldo A. 2003. On the drainage density of tidal networks. *Water Resources Research* **39**. DOI:10.1029/2001wr001051.

McDonnell JJ. 1990. A rationale for old water discharge through macropores in a steep, humid catchment. *Water Resources Research* **26**: 2821–2832. DOI:10.1029/WR026i011p02821.

McDonnell JJ, Beven K. 2014. Debates – the future of hydrological sciences: a (common) path forward? A call to action aimed at understanding velocities, celerities and residence time distributions of the headwater hydrograph. *Water Resources Research* **50**: 5342–5350. DOI:10.1002/2013WR015141.

Mesa O, Mifflin E. 1986. On the relative role of hillslope and network geometry in hydrologic response. In *Scale Problems in Hydrology*, Gupta V, Rodríguez-Iturbe I, Wood EF (eds). Springer: Netherlands **6**: 1–17. DOI: 10.1007/978-94-009-4678-1_1

Montgomery DR, Dietrich WE. 1992. Channel initiation and the problem of landscape scale. *Science* **255**: 826–830. DOI:10.1126/science.255.5046.826.

Montgomery DR, Foufoula-Georgiou E. 1993. Channel network source representation using digital elevation models. *Water Resources Research* **29**(12): 3925–3934. DOI:10.1029/93wr02463.

Mutzner R, Bertuzzo E, Tarolli P, Weijs SV, Nicotina L, Ceola S, Tomasic N, Rodriguez-Iturbe I, Parlange MB, Rinaldo A. 2013. Geomorphic signatures on Brutsaert base flow recession analysis. *Water Resources Research* **49**: 5462–5472. DOI:10.1002/wrcr.20417.

Mutzner R, Weijs SV, Tarolli P, Calaf M, Oldroyd HJ, Parlange MB. 2015. Controls on the diurnal streamflow cycles in two sub-basins of an alpine headwater catchment. *Water Resources Research* **51**: 3043–3418. DOI:10.1002/2014WR016581.

Nadeau DF, Pardyjak ER, Higgins CW, Huwald H, Parlange MB. 2012. Flow during the evening transition over steep Alpine slopes. *Quarterly Journal of the Royal Meteorological Society* **139**(672): 607–624. DOI:10.1002/qj.1985.

Nardi F, Grimaldi S, Santini M, Petroselli A, Ubertini L. 2008. Hydrogeomorphic properties of simulated drainage patterns using digital elevation models: the flat area issue. *Hydrological Sciences Journal* **53**: 1176–1193. DOI:10.1623/hysj.53.6.1176.

O'Callaghan JF, Mark DM. 1984. The extraction of drainage networks from digital elevation data. *Computer Vision, Graphics, and Image Processing* **28**: 323–344. DOI:10.1016/s0734-189x(84)80011-0.

Oldroyd HJ, Katul G, Pardyjak ER, Parlange MB. 2014. Momentum balance of katabatic flow on steep slopes covered with short vegetation. *Geophysical Research Letters* **41**(13): 4761–4768. DOI:10.1002/2014GL060313.

Orlandini S, Moretti G, Franchini M, Aldighieri B, Testa B. 2003. Path-based methods for the determination of nondispersive drainage directions in grid-based digital elevation models. *Water Resources Research* **3**. DOI:10.1029/2002WR001639.

Orlandini S, Tarolli P, Moretti G, Dalla FG. 2011. On the prediction of channel heads in a complex alpine terrain using gridded elevation data. *Water Resources Research* **47**. DOI:10.1029/2010WR009648.

Passalacqua P, Tarolli P, Foufoula-Georgiou E. 2010a. Testing space-scale methodologies for automatic geomorphic feature extraction from lidar in a complex mountainous landscape. *Water Resources Research* **46**. DOI:10.1029/2009WR008812.

Passalacqua P, Do Trung T, Foufoula-Georgiou E, Sapiro G, Dietrich WE. 2010b. A geometric framework for channel network extraction from lidar: nonlinear diffusion and geodesic paths. *Journal of Geophysical Research, Earth Surface* **115**(15). DOI:10.1029/2009JF001254.

Petroselli A. 2012. LIDAR data and hydrological applications at the basin scale. *GIScience & Remote Sensing* **49**: 139–162. DOI:10.2747/1548-1603.49.1.139.

Pirotti F, Tarolli P. 2010. Suitability of LiDAR point density and derived landform curvature maps for channel network extraction. *Hydrological Processes* **24**: 1187–1197. DOI:10.1002/hyp.7582.

Quinn P, Beven K, Chevallier P, Planchon O. 1991. The prediction of hillslope flow paths for distributed hydrological modelling using digital terrain models. *Hydrological Processes* **5**: 59–79. DOI:10.1002/hyp.3360050106.

Rinaldo A, Vogel GK, Rigon R, Rodriguez-Iturbe I. 1995. Can one gauge the shape of a basin? *Water Resources Research* **31**: 1119–1127. DOI:10.1029/94wr03290.

Schaefli B, Nicótina L, Imfeld C, Da Ronco P, Bertuzzo E, Rinaldo A. 2014. SEHR-ECHO v1.0: a spatially-explicit hydrologic response model for ecohydrologic applications. *Geoscientific Model Development Discussions* **7**: 1865–1904. DOI:10.5194/gmdd-7-1865-2014.

Simoni S, Zanotti F, Bertoldi G, Rigon R. 2008. Modelling the probability of occurrence of shallow landslides and channelized debris flows using GEOtop-FS. *Hydrological Processes* **22**: 532–545. DOI:10.1002/hyp.6886.

Simoni S, Padoan S, Nadeau DF, Diebold M, Porporato A, Barrenetxea G, Ingelrest F, Vetterli M, Parlange MB. 2011. Hydrologic response of an alpine watershed: application of a meteorological wireless sensor network to understand streamflow generation. *Water Resources Research* **47**(10). DOI:10.1029/2011wr010730.

Singh P, Mishra S, Jain MK. 2014. A review of the synthetic unit hydrograph: from the empirical UH to advanced geomorphological methods. *Hydrological Sciences Journal* **59**: 239–261. DOI:10.1080/02626667.2013.870664.

Sofia G, Tarolli P, Cazorzi F, Dalla Fontana G. 2011. An objective approach for feature extraction: distribution analysis and statistical descriptors for scale choice and channel network identification. *Hydrology and Earth System Sciences* **15**: 1387–1402. DOI:10.5194/hess-15-1387-2011.

Sofia G, Pirotti F, Tarolli P. 2013. Variations in multiscale curvature distribution and signatures of LiDAR DTM errors. *Earth Surface Processes and Landforms* **38**: 1116–1134. DOI:10.1002/esp.3363.

Sofia G, Tarolli P, Cazorzi F, Dalla Fontana G. 2015. Downstream hydraulic geometry relationships: gathering reference reach-scale width values from LiDAR. *Geomorphology* **250**: 236–248. DOI:10.1016/j.geomorph.2015.09.002.

Szilágyi J, Parlange MB. 1999. A geomorphology-based semi-distributed watershed model. *Advances in Water Resource* **23**: 177–187. DOI:10.1016/S0309-1708(99)00021-4.

van der Tak LD, Bras RL. 1990. Incorporating hillslope effects into the geomorphologic instantaneous unit hydrograph. *Water Resources Research* **26**: 2393–2400. DOI:10.1029/WR026i010p02393.

Tarboton D. 1997. A new method for the determination of flow directions and upslope areas in grid digital elevation models. *Water Resources Research* **33**: 309–319. DOI:10.1029/96wr03137.

Tarolli P. 2014. High-resolution topography for understanding Earth surface processes: opportunities and challenges. *Geomorphology* **216**: 295–312. DOI:10.1016/j.geomorph.2014.03.008.

Tarolli P, Dalla Fontana G. 2009. Hillslope-to-valley transition morphology: new opportunities from high resolution DEMs. *Geomorphology* **113**: 47–56. DOI:10.1016/j.geomorph.2009.02.006.

Tarolli P, Sofia G, Dalla Fontana G. 2012. Geomorphic features extraction from highresolution topography: landslide crowns and bank erosion. *Natural Hazards* **61**: 65–83. DOI:10.1007/s11069-010-9695-2.

Troutman BM, Karlinger MR. 1985. Unit hydrograph approximations assuming linear flow through topologically random channel networks. *Water Resources Research* **21**: 743–754. DOI:10.1029/WR021i005p00743.

Tucker GE, Catani F, Rinaldo A, Bras RL. 2001. Statistical analysis of drainage density from digital terrain data. *Geomorphology* **36**: 187–202. DOI:10.1016/S0169-555X(00)00056-8.

Weijs SV, Mutzner R, Parlange MB. 2013. Could electrical conductivity replace water level in rating curves for alpine streams? *Water Resources Research* **49**(1). DOI:10.1029/2012WR012181.

Yokoyama R, Sirasawa M, Pike R. 2002. Visualizing topography by openness: a new application of image processing to digital elevation models. *Photogrammetric Engineering & Remote Sensing* **68**(3): 257–265.

Zoccatelli D, Borga M, Zanon F, Antonescu B, Stancalie G. 2010. Which rainfall spatial information for flash flood response modelling? A numerical investigation based on data from the Carpathian range, Romania. *Journal of Hydrology* **394**: 148–161. DOI:10.1016/j.jhydrol.2010.07.019.

